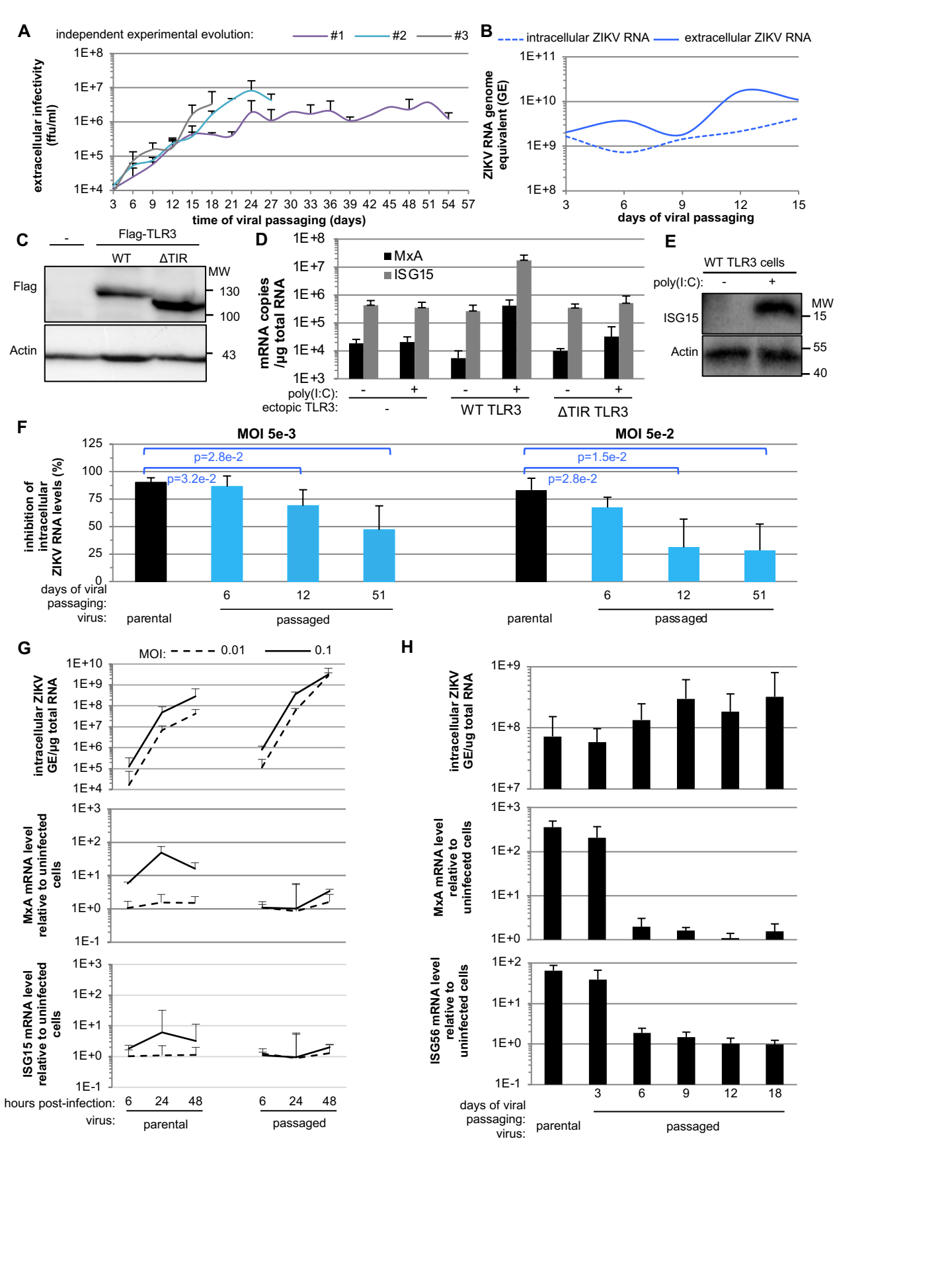
A
independent experimental evolution:
#1
#2
#3
extracellular infectivity (ffu/ml)
1E+8
1E+7
1E+6
1E+5
1E+4
3 6 9 12 15 18 21 24 27 30 33 36 39 42 45 48 51 54 57
time of viral passaging (days)
B
intracellular ZIKV RNA
extracellular ZIKV RNA
ZIKV RNA genome equivalent (GE)
1E+11
1E+10
1E+9
1E+8
3 6 9 12 15
days of viral passaging
C
-
Flag-TLR3
WT
ΔTIR
MW
Flag
130
100
Actin
43
D
MxA
ISG15
mRNA copies /µg total RNA
1E+8
1E+7
1E+6
1E+5
1E+4
1E+3
poly(I:C):
ectopic TLR3:
-
WT TLR3
ΔTIR TLR3
E
WT TLR3 cells
poly(I:C):
ISG15
Actin
MW
15
55
40
F
MOI 5e-3
MOI 5e-2
p=2.8e-2
p=3.2e-2
p=1.5e-2
p=2.8e-2
inhibition of intracellular ZIKV RNA levels (%)
125
100
75
50
25
0
days of viral passaging:
virus:
parental
6
12
51
passaged
G
MOI:
0.01
0.1
intracellular ZIKV GE/µg total RNA
1E+10
1E+9
1E+8
1E+7
1E+6
1E+5
1E+4
MxA mRNA level relative to uninfected cells
1E+3
1E+2
1E+1
1E+0
1E-1
ISG15 mRNA level relative to uninfected cells
hours post-infection:
6
24
48
virus:
parental
passaged
H
intracellular ZIKV GE/ug total RNA
1E+9
1E+8
1E+7
MxA mRNA level relative to uninfecetd cells
1E+3
1E+2
1E+1
1E+0
ISG56 mRNA level relative to uninfected cells
1E+2
1E+1
1E+0
1E-1
3
6
9
12
18
days of viral passaging:
virus:
parental
passaged

Supplementary Figure 1. Validation of cell study model and analysis of the replication and ISG response upon infection by parental virus and passaged viral populations. A. Quantification of the extracellular infectivity of the viral populations harvested over serially passaging in the course of 3 independent run of experimental evolution (referred to as #1, #2, #3 and stop at days 54, 21 and 18 respectively). Results are expressed as foci forming unit (ffu/ml); determined by 2-to-3 independent measurements for each independent run of experimental evolution; mean ± SD. **B.** Quantification of extracellular and intracellular ZIKV genome (genome equivalent; GE) levels in serial passaging of viral populations by RT-qPCR, results of replicate #1. **C.** Western blot analysis of ectopic WT and ΔTIR TLR3 expression in Huh7.5.1 cells, and as reference the parental Huh7.5.1 cells (-). WT and ΔTIR TLR3 are detected by their Flag-tag; actin detection used as loading control. **D-E**. Analysis of MxA and ISG15 induction upon treatment by poly(I:C) at 100 µg/ml by quantification of MxA and ISG15 mRNA levels by RT-qPCR (**D**) and western blot (**E**). **F.** Inhibition by TLR3-signaling of replication of viral populations harvested at the indicated times of the serial passaging (i.e., day 6, 12 and 51). Results represent the percentage of inhibition in activated-TLR3 cells relative to control cells of intracellular ZIKV genome levels determined at 3 days post-infection at MOI 5e-3 (left panel) and 5e-2 (right panel); 4 independent experiments; mean ± SD; significant differences ($p<0.05$) are indicated by the brackets the top of the graphs. **G.** Quantification of the intracellular ZIKV RNA (upper panel), MxA (middle panel) and ISG15 mRNA (lower panel) levels at the indicated time points post-infection of Huh7.5.1 cells by parental virus and viral populations harvested at day 36 of the viral passaging, as indicated. Infection were performed at MOI 0.1 and 0.01; 3 independent experiments; mean ± SD. **H.** Quantification of the intracellular ZIKV RNA (upper panel), MxA (middle panel) and ISG56 (lower panel) mRNA levels at 24 hours post-infection by viral populations harvested at the indicated times of the serial passaging viral population and parental virus. Infections performed at MOI 1; 3 independent experiments; mean ± SD.

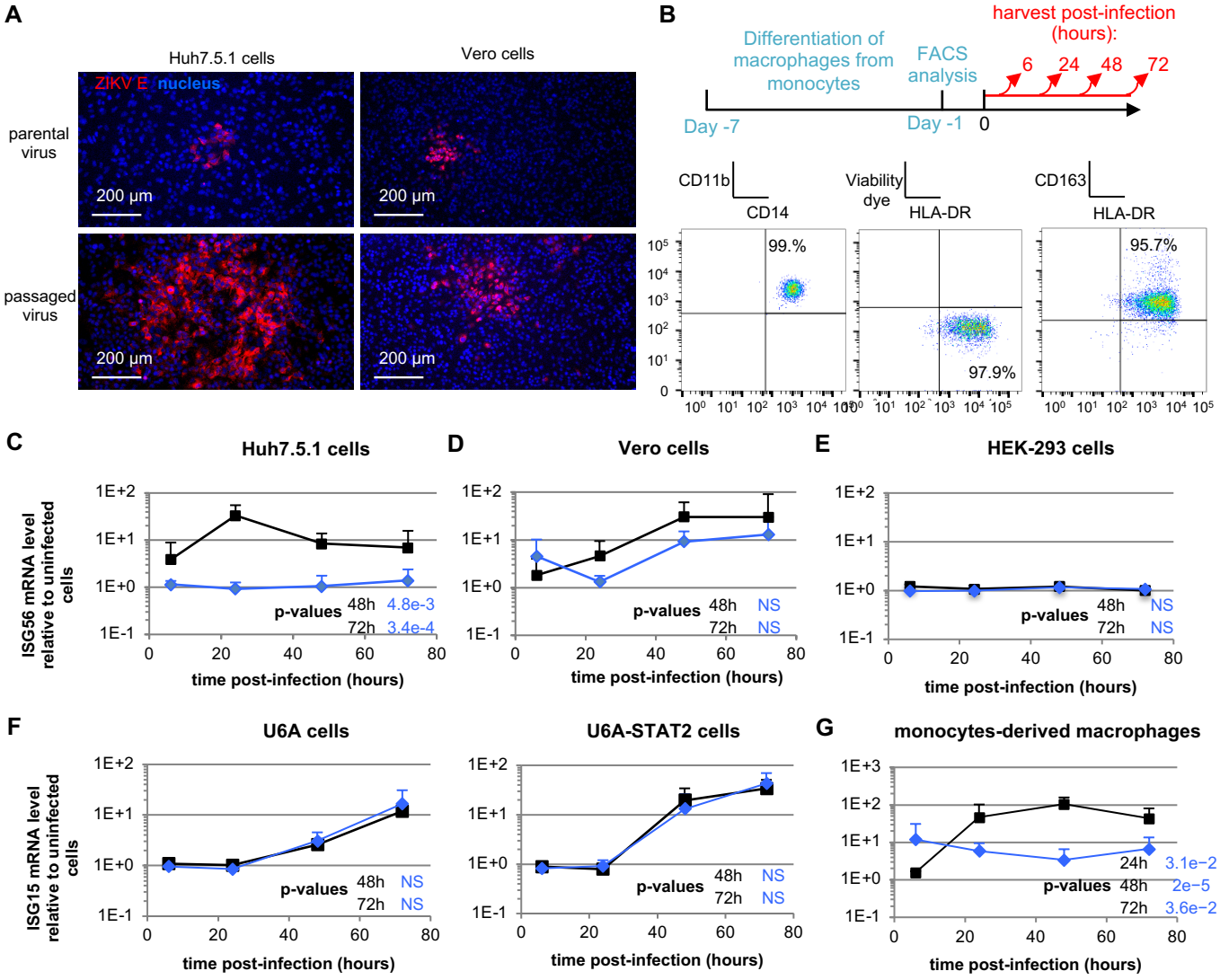

Supplementary Figure 2. Comparison of viral replication of the passaged viral population in various cell lines. A. Representative imaging of infectious foci at 48 hours post-infection by parental virus *versus* serially passaged virus (*i.e.,* day 51 of the viral passaging) in Huh7.5.1 cells (right panels) and Vero cells (left panels) by immunostaining of E enveloppe proteins (red); nucleus stained by Hoechst (blue); scale-bar indicated. **B.** Upper panel, schematic representation of the experimental timeline for macrophages derived from monocytes and infection. Lower panels, their differentiation levels were determined by FACS at the day prior infection and using CD11b, CD14, HLA-DR, CD163 differentiqtion marker and viability markers, as indicated; representative of 4 independent experiments. **C-G.** Kinetic quantification of ISG56 mRNA levels relative to the levels in non-infected cells, at the indicated time post-infection at MOI 0.1 by parental virus versus serially passaged viral population (*i.e.,* day 51 of the viral passaging) in Huh7.5.1 (**C**), Vero cells (**D**), HEK293 cells (**E**), U6A cells and STAT2 expressing U6A cells (**F**), and macrophages derived from monocytes (**G**). 3-to-7 independent experiments; mean ± SD. The p-values of the statistical analysis of the kinetics performed using mixed linear model are indicated on the right side of the graphs, p-value are for the comparison of passaged viral population versus parental virus, and NS; p>0.05.

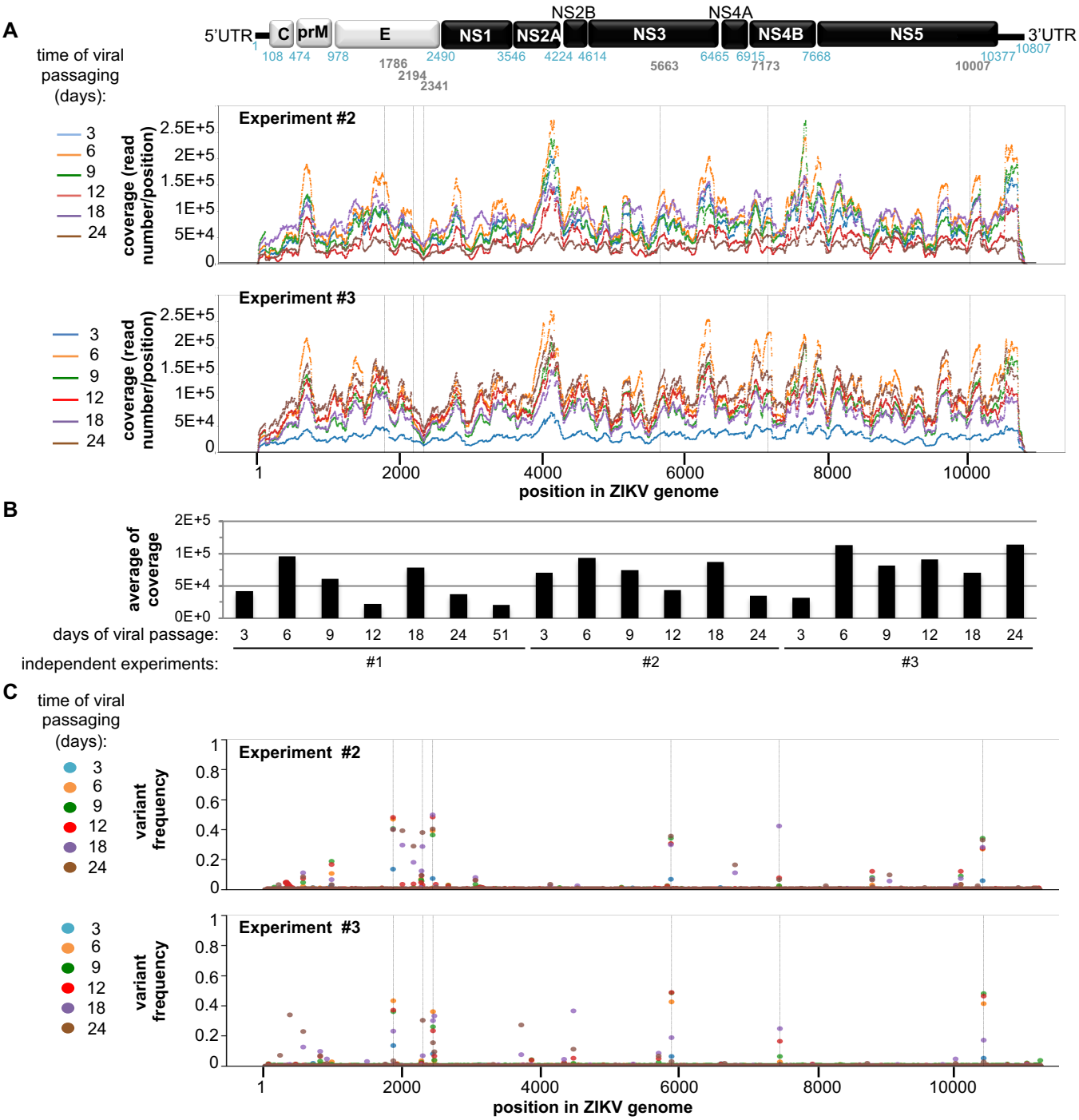

Supplementary Figure 3. Bioinformatic analysis of the genetic evolution of viral populations obtained by next-generation sequencing. A. Coverage of the next-generation sequencing analysis along the ZIKV genome sequence of viral populations harvested at the indicated time points of the serial passaging of independent run of evolution experiment #2 and #3. Schematic representation of ZIKV genome at the top. **B.** Average coverage of the sequenced ZIKV genome for the serially passaged viral population contained in supernatants harvested at the indicated time-points and for independent runs of evolution experiment. **C.** Time-course quantification of the frequency of the second most frequent variants at each position along ZIKV genome in the viral populations harvested in independent runs of evolution experiment #2 and #3. Dotted lines indicate the positions in the viral genome with high standard deviations in several runs of experimental evolution, as defined in **Fig S4A**.

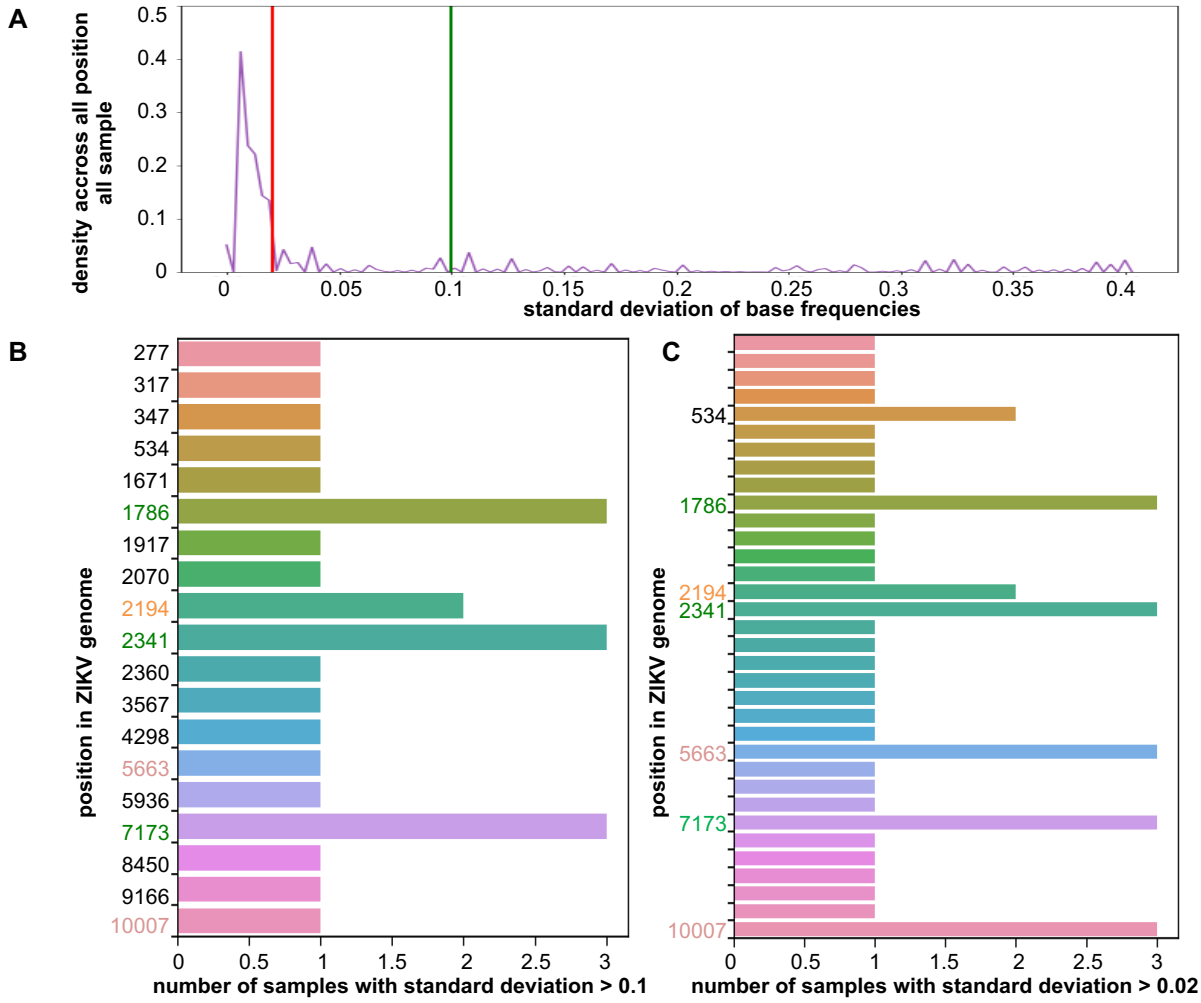

Supplementary Figure 4. Bioinformatics analysis leading to the selection of candidate adaptive mutations. A. Distribution of the standard deviations of variant frequencies across all analyzed samples. Thresholds at 0.02 (red line) and 0.1 (green line) are used for the selection of variants of interest. **B-C.** Representation of the number of samples where a given variant is above the standard deviation of 0.1 (**B**) and 0.02 (**C**) across ZIKV genome.

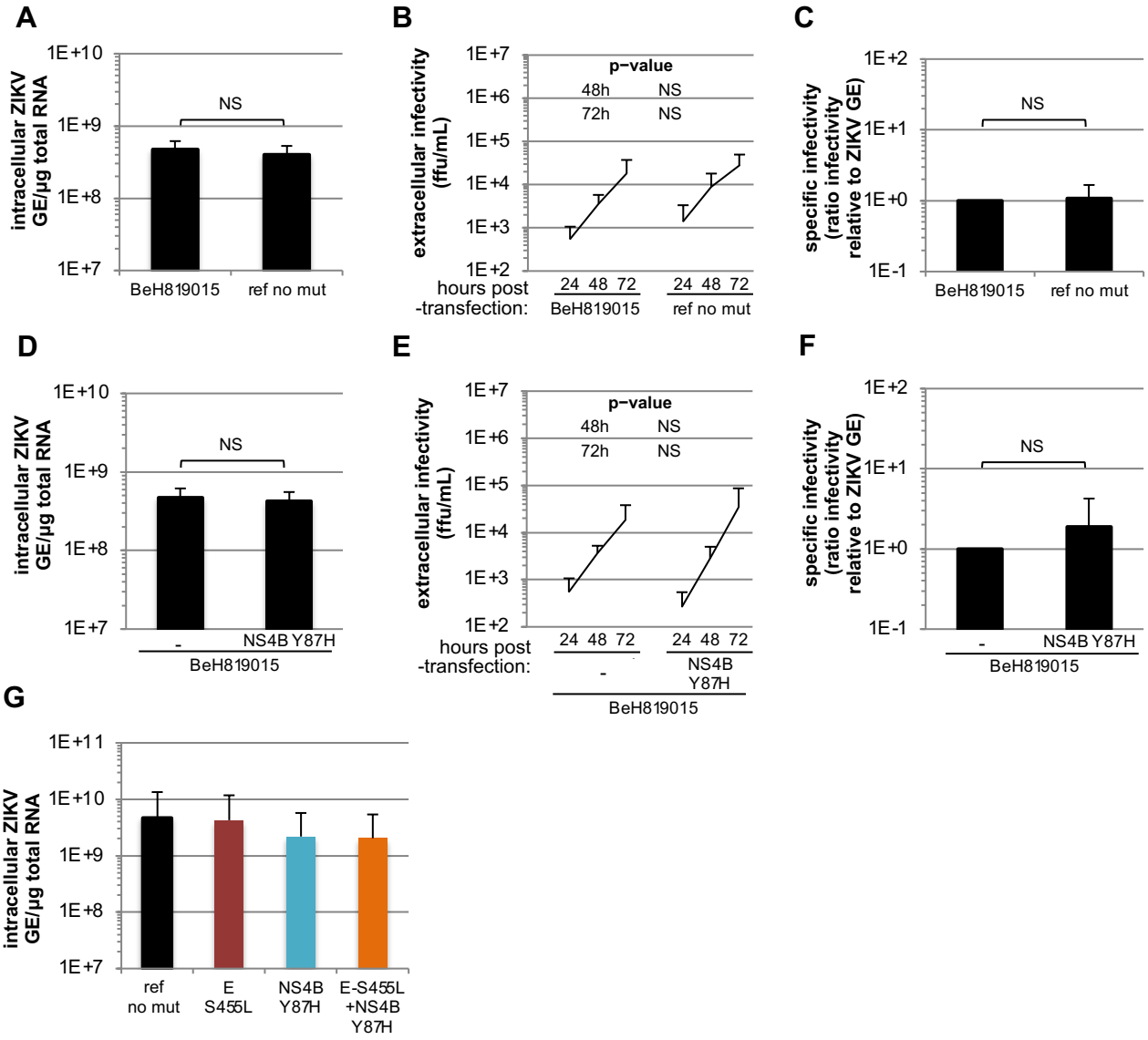
A
intracellular ZIKV GE/µg total RNA
1E+10
1E+9
1E+8
1E+7
NS
BeH819015
ref no mut
B
extracellular infectivity (ffu/mL)
1E+7
1E+6
1E+5
1E+4
1E+3
1E+2
p-value
48h NS
72h NS
hours post -transfection:
24 48 72
24 48 72
BeH819015
ref no mut
C
specific infectivity (ratio infectivity relative to ZIKV GE)
1E+2
1E+1
1E+0
1E-1
NS
BeH819015
ref no mut
D
intracellular ZIKV GE/µg total RNA
1E+10
1E+9
1E+8
1E+7
NS
-
NS4B Y87H
BeH819015
E
extracellular infectivity (ffu/mL)
1E+7
1E+6
1E+5
1E+4
1E+3
1E+2
p-value
48h NS
72h NS
hours post -transfection:
24 48 72
24 48 72
-
NS4B Y87H
BeH819015
F
specific infectivity (ratio infectivity relative to ZIKV GE)
1E+2
1E+1
1E+0
1E-1
NS
-
NS4B Y87H
BeH819015
G
intracellular ZIKV GE/µg total RNA
1E+11
1E+10
1E+9
1E+8
1E+7
ref no mut
E S455L
NS4B Y87H
E-S455L +NS4B Y87H
H
ref no mut
Huh7.5.1 cells
Vero cells
E S455L
Huh7.5.1 cells
Vero cells
ZIKV E nucleus
200 µm
200 µm
200 µm
200 µm
NS4B Y87H
Huh7.5.1 cells
Vero cells
E S455L+NS4B Y87H
Huh7.5.1 cells
Vero cells
ZIKV E nucleus
200 µm
200 µm
200 µm
200 µm

Supplementary Figure 5. Validation of ZIKV molecular clone used for the introduction of the selected non-synonymous mutations in ZIKV molecular clone. A-C. The BeH819015 ZIKV molecular clone (referred to as BeH819015) and derived clones with NS1 mutation, used as reference in **Fig 3** ("ref no mut") were transfected in Huh7.5.1 cells. **A.** Comparable transfection efficiency was assessed by quantification of the intracellular ZIKV GE levels at 6 hours post-transfection; 3 independent experiments; mean ± SD; no statistical difference. **B**. Time-course quantification of infectious viral production at the indicated times post-transfection; 4 independent experiments; mean ± SD; no significant difference as indicated in the table above the graph. **C.** Quantification of the specific infectivity in viral supernatants harvested at 72 hours post-transfection of the indicated molecular clones. Results represent the ratio of the extracellular infectivity relative to extracellular ZIKV RNA levels as in **Fig. 1A**. Results present mean ± SD of 4 independent experiments and set to 1 for BeH819015 for each independent analysis; no significant difference of viral spread overtime as indicated above the graph. **D-F.** The BeH819015 ZIKV molecular clone without mutation (-) versus NS4B Y87H mutation introduce in the same background (referred to as BeH819015) were transfected in Huh7.5.1 cells. Results displayed as in panels **A-C;** 3 independent experiments for panel D and 4 independent experiments for panels **E-F**; mean ± SD; no statistical difference. **G.** ZIKV genome bearing the selected mutations (*i.e.,* single S455L mutation in E, Y87H in NS4B and combined E S455L and NS4B Y87H mutations), and as a reference ZIKV genome without the mutation ("ref no mut"), were transfected in Huh7.5.1 cells. Similar transfection efficiencies were assessed by quantification of the intracellular ZIKV GE levels at 6 hours post-transfection (relative to **Fig. 3A**); 5 independent experiments; mean ± SD; no statistical differences. **H.** Representative imaging of infectious foci at 48 hours post-infection of ZIKV bearing the single S455L mutation in E, Y87H in NS4B and combined E S455L and NS4B Y87H mutations, and as a reference the ZIKV genome without these mutations ("ref no mut") in Huh7.5.1 cells, performed as in **Fig. 3C**; immunostained E surface proteins (red); nucleus stained by Hoechst (blue); scale-bar indicated.

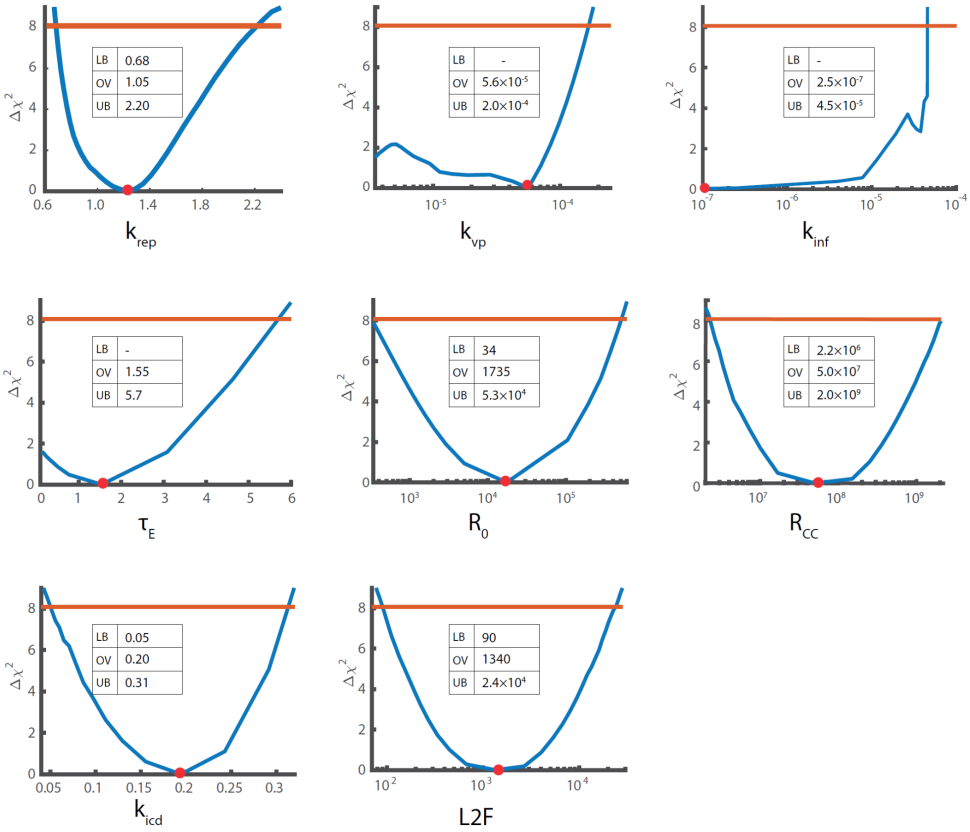

Supplementary Figure 6. Parameter identification. The 95% confidence intervals for the estimated parameter values were calculated using the profile-likelihood method (**Appendix 1**, mathematical model). The blue curve is the maximum-likelihood profile, the solid red line shows the 95% threshold and the red circle represents the estimated parameter value. The estimated parameter values are reported together with their 95% confidence bounds when the parameter is bounded; LB; lower bound, OV; optimal value and UB; upper bound of the respective parameters.

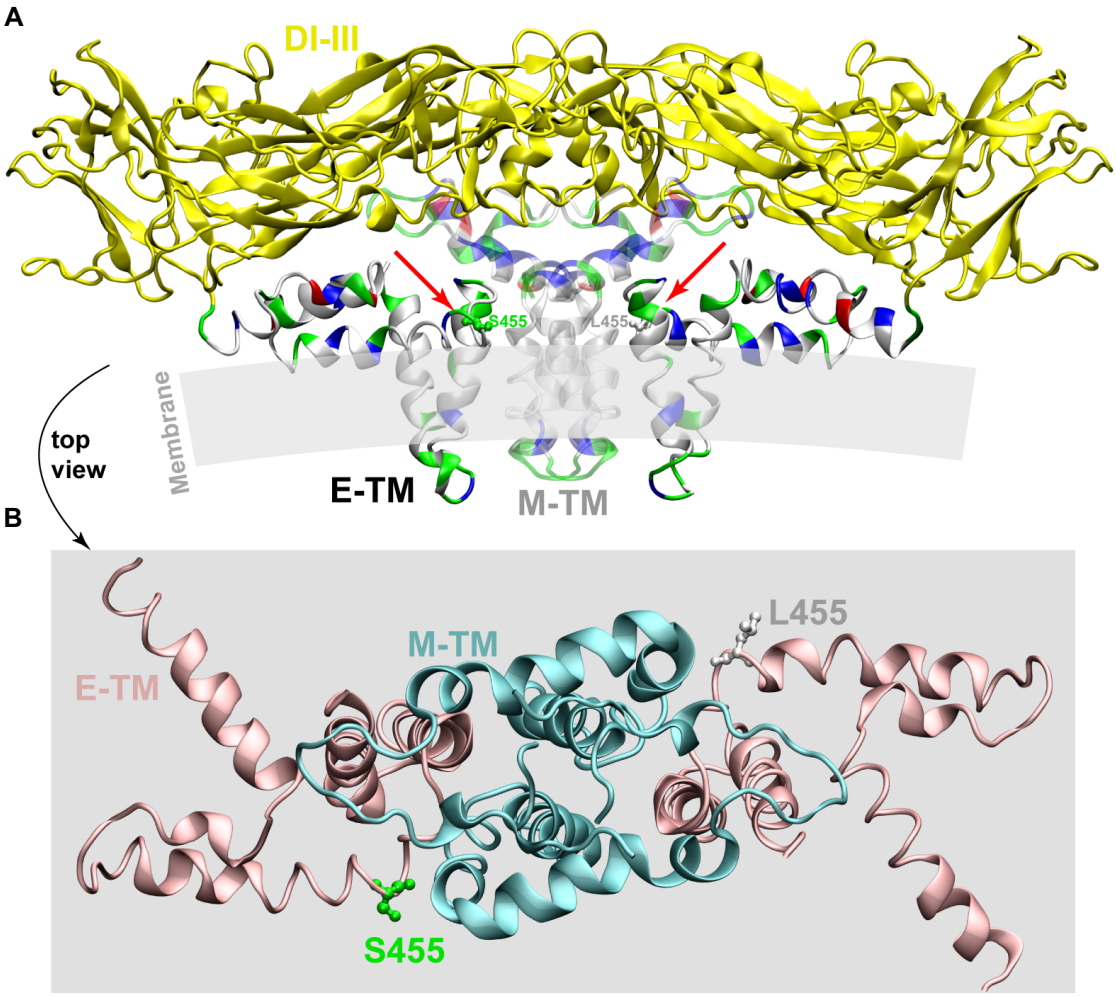

Supplementary Figure 7. Positioning of the S455L mutation in E structure. A. Structure of ZIKA E (in solid) and M (transparent) proteins (5IRE.pdb) (44), with EI-III domains forming the envelope shell (yellow). The E and M protein transmembrane (TM) domains are shown with residue types indicated on the structure (white, hydrophobic; green, polar; bleu, basic; red, acidic) in order to locate membrane insertion and to point out (red arrows) the positions of S455 (left monomer) and the mutant form L455 (right monomer) at the membrane interface. **B.** Zoom of E-TM (cyan) and M-TM (pink), without EI-III, as view from the top of the structure shown in (**A**). The positions of the wild-type S455 and mutant L455 residues at the interface between E and M TM domains are shown on one monomer each (the orientation of the L455 side chain is arbitrary), and has been created using the mutation tool in Swiss-PdbViewer.